ACS Catalysis

pubs.acs.org/acscatalysis

Research Article

Effect of Nanoparticle Ligands on 4-Nitrophenol Reduction: Reaction Rate, Induction Time, and Ligand Desorption

Robert D. Neal, Robert A. Hughes, Pitambar Sapkota, Sylwia Ptasinska, and Svetlana Neretina*

Cite This: *ACS Catal.* 2020, 10, 10040−10050

Read Online

ACCESS | Metrics & More | Article Recommendations | Supporting Information

ABSTRACT: Ligands are the quintessential synthesis tool in the preparation of colloidal metal catalysts, allowing for the rational design of nanostructured surfaces with high activity and selectivity. These same agents can, however, strongly influence the catalytic performance of metal nanostructures in aqueous media. In this regard, the current literature describing the influence of ligands on the model catalytic reaction that sees 4-nitrophenol reduced to 4-aminophenol by borohydride is highly fragmented in that the understanding of reaction rate, induction time, and ligand desorption phenomena is disconnected and, at times, contradictory. Herein, we present a study in which three chemically distinct ligands are applied to bare gold catalysts followed by their exposure to aqueous solutions of relevance to 4-nitrophenol reduction while simultaneously tracking the ligand whereabouts. It is shown that the exposure of ligands to borohydride leads to their near-complete removal from the gold catalyst. This, in turn, gives rise to severe disruptions to the rate of 4-nitrophenol reduction for the scenario where the aqueous reactants are purged of dissolved oxygen and ligand desorption times are slow. In sharp contrast, the reaction rate is little affected when the same reactants contain dissolved oxygen because the resulting induction period provides ample time for the ligands to desorb prior to the onset of the reaction. Moreover, strongly bound ligands are shown to give rise to an induction-time-like feature that is only observable when the reactants are free of dissolved oxygen. Collectively, these findings advocate procedures for catalytic benchmarking that differ from current best practices and underscore the point that a fundamental understanding of 4-nitrophenol catalysis must adopt a holistic approach that accounts for ligand−nanostructure interdependencies.

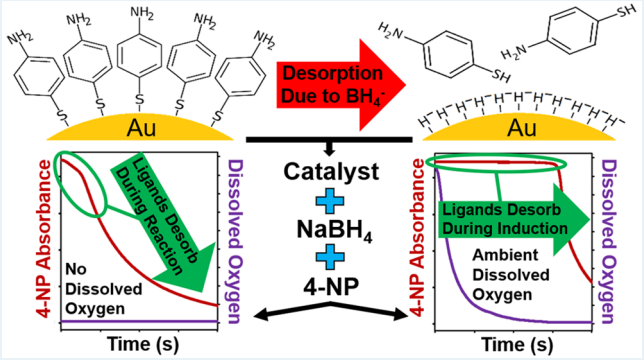

KEYWORDS: *4-nitrophenol, model reaction, ligands, dissolved oxygen, desorption, induction time*

INTRODUCTION

Surface ligands are an inherent component of colloidal chemistry, offering precise atomic control over nanostructure synthesis while ensuring long-term stabilization against agglomeration and aggregation.[1,2] As capping agents, ligands promote facet-selective growth and can assert control over such factors as composition, size, shape, and crystal structure.[2] Some capping ligands are additionally able to influence the kinetic and thermodynamic stability of the precursor metal complex or even act as a reducing agent, affecting the driving force for reduction and influencing the nanocrystal nucleation for self-seeded growths.[3] Capping ligands, which can take on many forms including organic molecules, ionic species, and macromolecules, collectively provide the synthetic tool that is able to tune structure−property relationships to fit the needs of specific applications. Nowhere is such a capability more valuable than it is in catalysis since the rational design of nanostructure contours frequently provide the means to facilitate a desired surface chemistry.

Although ligands are essential to the design and preservation of nanostructured catalysts, their influence on catalytic turnover in aqueous reactions can become obfuscated by competing factors. Ligands attached at the surface of nanostructures would seemingly be expected to inhibit catalytic activity because they block access to potentially active sites on the catalyst surface.[4−10] In accordance with this expectation, numerous studies have observed such negative impacts on catalytic rates.[4,5,7,11−14] Some studies, however, have observed no deleterious effects from capping ligands,[15−17] while others show increased selectivity toward certain reaction products,[18,19] indicating that benefit can be derived from complex chemical pathways involving ligand interactions.

Received: June 23, 2020
Revised: August 9, 2020
Published: August 10, 2020

https://dx.doi.org/10.1021/acscatal.0c02759
ACS Catal. 2020, 10, 10040−10050

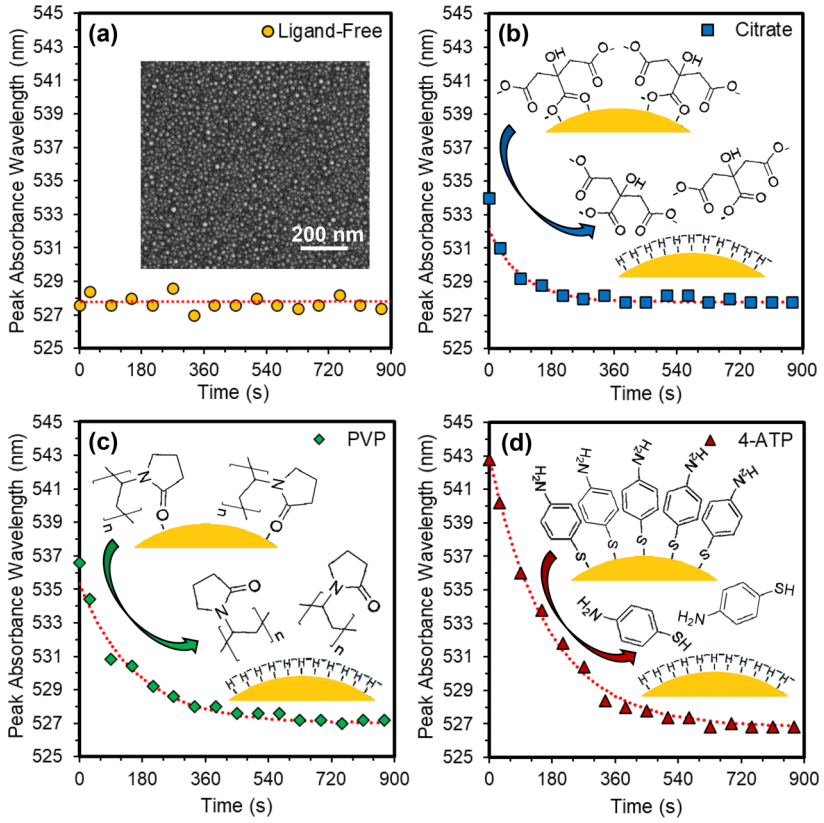

Figure 1. Time dependence of the LSPR wavelength of substrate-immobilized Au nanostructures obtained when submerged in aqueous $NaBH_4$ for structures that are (a) ligand-free and to which (b) citrate, (c) PVP, and (d) 4-ATP ligands are adsorbed. The various insets show an SEM image of the nanostructures used and schematics of the ligand exchange process that sees the starting ligand displaced by a hydrogen species derived from BH_4^-. The dashed red lines are fits to first order kinetics.

Regardless of whether harm or benefit occurs, these studies point toward the need to reconcile the observed turnover with the entire ligand−nanostructure system.

The reduction of 4-nitrophenol (4-NP) to 4-aminophenol (4-AP) by borohydride (BH_4^-) is a widely used model reaction for assessing the catalytic activity of nanostructures in aqueous media.[20−22] For this reaction, heterogeneous catalysts are benchmarked by spectroscopically monitoring the decline in the 400 nm 4-nitrophenolate ($4\text{-}NP^-$) absorbance peak after which an apparent reaction rate constant, k_{app}, is extracted from the linear slope of the $-\ln(A/A_0)$ versus time plot, where A/A_0 is the normalized $4\text{-}NP^-$ absorbance.[20] The procedure is simple, requires minimal instrumentation, and allows for straightforward data analysis. This model catalytic reaction has nevertheless become the subject of increasing scrutiny in terms of both the mechanistic framework required for its understanding and potential pitfalls that can lead to inaccurate or misleading results. Mechanistically, the reaction has been widely described in terms of the Langmuir−Hinshelwood model,[23−25] but others have argued in favor of the Eley−Rideal mechanism.[26−28] Severe disruptions to the reaction can also be caused by dissolved oxygen within the aqueous reactants in that it can lead to an induction time,[29−31] severely reduced k_{app} values,[32] and the oxidative etching of catalysts where, for certain cases, it is possible for the leached ions to give rise to a far more catalytically active species.[32] The induction time, which is a time interval at the beginning of the reaction where no turnover is observed, has proven particularly contentious. Current evidence, however, points toward the need for a side reaction that acts in opposition to 4-NP reduction,[29,30] in which a 4-nitrosophenol (4-NO) intermediate is oxidized back into 4-NP by dissolved oxygen.[31] The conclusion is supported by measurements that show that the removal of dissolved oxygen from the reaction solution using an inert gas purge eliminates the induction time while a continuous O_2 gas purge extends it indefinitely.[29]

The influence of ligands on the catalytic reduction of 4-NP is a complex subject due to the diverse range of ligands applied to nanostructures and the inability of characterization tools to accurately map out their number and arrangement on catalytic surfaces. As such, the current literature details numerous ligand influences that together form a convoluted and often contradictory commentary. Various studies have shown that ligands can increase, decrease, and have essentially no influence on k_{app}.[4,6,7,33−39] One investigation concluded that increases to the chain length of surface ligands increased catalytic activity[4] while other studies observed the opposite effect.[6,35] Numerous studies have shown that ligands can drastically alter the induction time, leading many to conclude that ligands, rather than dissolved oxygen, are its root cause.[4,5,14,35,37,40,41] Other reports have disputed this conclusion.[24] What is most perplexing is the near-complete disconnect between the 4-NP literature and the work of Ansar et al.[42] showing that $NaBH_4$, a reactant in the catalytic reduction of 4-NP, acts as a "general-purpose detergent" capable of displacing stabilizing ligands from nanoparticle surfaces. With subsequent studies confirming that $NaBH_4$ is able to remove common capping agents such as citrate,[4] polyethylene glycol (PEG),[4] polyvinylpyrrolidone (PVP),[5,43−46] and even difficult to remove thiols[4,45,47−50] at BH_4^- concentrations of relevance to 4-NP

https://dx.doi.org/10.1021/acscatal.0c02759
ACS Catal. 2020, 10, 10040−10050

reduction (i.e., 1−100 mM), it follows that such influences are prevalent when benchmarking catalysts. Several 4-NP studies have notably acknowledged the $NaBH_4$ "detergent effect" on 4-NP catalysis,[4,5] yet a thorough investigation has not hitherto been carried out.

Numerous studies directed toward elucidating the mechanistic understanding of 4-NP reduction and the intrinsic reaction kinetics associated with specific nanomaterials have employed ligand-free catalysts so as to eliminate the confounding effects of capping agents.[51−58] In our prior work,[29,30,32,54] we have used both substrate-supported and borohydride-protected metal catalysts for this purpose where the latter can be considered ligand-free because it utilizes BH_4^- (an ion already present in large excess in 4-NP reduction) as the stabilization agent.[59] The availability of these ligand-free catalysts provide an intriguing testbed for studying ligand effects in that various capping agents can be attached to these bare catalysts so as to compare their catalytic activity with and without these surface agents. Herein, we present the results of an investigation that delineates the influence of three widely used capping agents on the catalytic reduction of 4-NP. It is shown that citrate, PVP, and 4-ATP (4-aminothiophenol) capped Au nanoparticles are all subject to the detergent effect but where the rate and means by which they desorb can dramatically influence the induction time and k_{app}. The results obtained demonstrate that the mechanistic influences of ligands are highly intertwined and sometimes masked by competing phenomenon but where the isolation of individual aspects allows for an understanding that can be rationalized within the context of much of the preceding literature.

RESULTS

Ligand Desorption from Au Nanostructures. It is well-established that ligand attachment to bare Au nanostructures results in a red shift in the localized surface plasmon resonance (LSPR) where the extent to which it shifts for any given ligand is dependent on such factors as its dielectric properties, surface coverage, and the degree to which it interacts with the Au surface.[60] It, therefore, follows that ligand desorption from the same structures give rise to a blue shift. Real-time UV−vis spectroscopic monitoring of this event, hence, provides an in situ diagnostic for ligand desorption kinetics. To achieve this outcome, ligand-free plasmonic nanostructures were first prepared by sputter depositing ultrathin Au films onto sapphire substrates and exposing them to a heating regimen that sees each self-assemble into a collection of near-hemispherical structures via solid-state dewetting.[61] The so-formed structures, shown in the inset to Figure 1a, are well-bonded to the substrate, have an average diameter of 10.8 nm, and exhibit a 525 nm plasmon resonance in air (Figure S1). Samples prepared in this manner were then submerged in a solution containing the capping ligand, incubated for 30 min, and rinsed. The procedure resulted in LSPR red shifts of 8, 10, and 16 nm when measured in air for the citrate, PVP, and 4-ATP ligands, respectively (Figures S2 and S3). Such samples provide an excellent platform for studying desorption kinetics because (i) the whereabouts of the ligands are known prior to BH_4^- exposure, (ii) only limited quantities of ligands are adsorbed on the small amount of Au present (m_{Au} = 4.25 μg), and (iii) ligand-free samples provide an excellent control for monitoring any changes to the Au LSPR that could arise from extraneous factors such as leaching. The data is obtained by placing a sample vertically in a cuvette and then exposing it to aqueous $NaBH_4$ (12.5 mL, 20 mM) while continuously acquiring absorption scans from which the time dependence of the LSPR center frequency can be extracted.

Figure 1 shows the time dependence of the LSPR wavelength for substrate-immobilized Au catalysts that are ligand-free and to which the various ligands are adsorbed. When exposed to aqueous $NaBH_4$, the ligand-free structures, as expected, show no variation in their LSPR over the duration of the measurement (Figure 1a). The result is also consistent with earlier work showing Au to be impervious to leaching when exposed to aqueous $NaBH_4$.[32] In contrast, the ligand-capped structures (Figure 1b−d) all show values that monotonically blue shift until they finally plateau at an LSPR value that is, within experimental uncertainty, identical with that obtained for the ligand-free sample. The implication of this result is that all three ligands are displaced from the nanostructure surface by a hydrogen species derived from BH_4^- that is known to act as an effective stabilizing agent for colloidal Au nanostructures.[54,59] Although numerous factors can come into play, it is noteworthy that the times required for ligand desorption, showing values of 3, 7, and 10 min for citrate, PVP, and 4-ATP, respectively, follow a well-documented bonding strength hierarchy. Citrate weakly bonds to Au[62] and is readily displaced by PVP in colloidal syntheses requiring ligand exchange,[63] while thiols are well-recognized for both their ability to displace PVP[63] and to form strong bonds with Au nanostructures.[10,42,64] The desorption time scales are also in good agreement with the prior work of Ansar et al.[42] that characterized the BH_4^- detergent effect using time-dependent surface enhanced Raman scattering (SERS). Also noteworthy is that the time dependence of the desorption process can be described in terms of first order kinetics (Figure S4) if it is assumed that the shift in the LSPR varies linearly with ligand loading, as has been observed for other systems.[65,66] Once removed from the BH_4^- and rinsed, the LSPR for each sample was measured again in air. The measurements reveal that all ligand-capped samples show a spectrum that is near-identical with that obtained before the ligands were applied but where for each case there is a slight red shift (Figure S3). The result provides further evidence that BH_4^- exposure leads to ligand removal.

X-ray photoelectron spectroscopy (XPS) was used to further verify and corroborate that ligands are removed from the surface of Au nanostructures when exposed to aqueous $NaBH_4$. The 4-ATP ligand was specifically targeted in these measurements because the strong Au−S bond formed at the nanostructure−ligand interface readily lends itself to XPS detection and is only present due to the ligand added, whereas citrate and PVP have an O-bond with the Au surface, making it difficult to distinguish the ligand−Au bond from carbonaceous contamination that commonly occurs at the Au surface.[67] Two identical samples were fabricated and capped with 4-ATP using the aforementioned procedures where one of them underwent immediate XPS characterization while the other was submerged in aqueous $NaBH_4$ (12.5 mL, 20 mM) for 15 min before XPS characterization. Together, these two samples provide before and after representations of the XPS spectra upon exposure to BH_4^-. Figure 2 shows the XPS spectra of S 2p and Au 4f core levels. The peak in S 2p spectra (Figure 2a) at 164 eV that arises from S atoms bonded to Au, while present before BH_4^- exposure, is absent afterward. This absence is a clear indication that the 4-ATP ligand has, as anticipated, been removed. Supporting this conclusion are the increased Au 4f

https://dx.doi.org/10.1021/acscatal.0c02759
ACS Catal. 2020, 10, 10040−10050

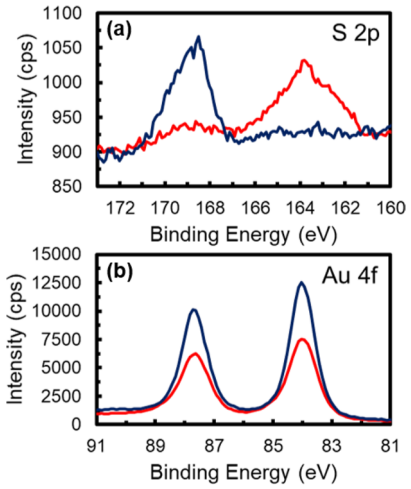

Figure 2. XPS core level spectra of (a) S 2p and (b) Au 4f obtained from 4-ATP-coated Au nanostructures before (red) and after (blue) exposure to aqueous BH_4^-.

peak intensities at 84 and 88 eV observed after BH_4^- exposure (Figure 2b), an increase that is anticipated if the attenuating influence of the ligand is absent. Although the origins of the peak at 169 eV appearing after BH_4^- exposure is unclear, its position is consistent with the formation of a sulfur−oxygen bond. The emergence of such a bond could indicate that 4-ATP removal results in the breakup of the 4-ATP molecule and the subsequent deposition of S on the exposed surface of the oxide substrate. These XPS results, in combination with the spectroscopic data, therefore indicate that BH_4^- exposure rids Au catalysts of their ligands with desorption times that are dependent on the ligand used.

Ligand Influences on 4-NP Catalysis. With the understanding that capping ligands desorb from Au catalysts, it may be anticipated that such an effect would minimize their influence on the catalytic reduction of 4-NP. This, however, is not the case because the desorption times needed are of relevance to the 4-NP induction time and the typical durations during which catalytic turnover occurs. Moreover, with the induction time dependent on catalytic activity[30,31] and the activity likely to be compromised by ligands, slow desorption processes could further delay the onset of the reaction. With the potential for such influences, the catalytic reduction of 4-NP was investigated using colloidal Au nanostructures synthesized using the Turkevich method[68,69] and a synthetic protocol forwarded by Deraedt et al.[59] The Turkevich method yields citrate-capped Au nanostructures but where ligand exchange processes allow for the substitution of citrate ligands with PVP or 4-ATP. The Deraedt protocol reduces Au^{3+} ions derived from $HAuCl_4$ with BH_4^- to form Au nanoparticles where excess BH_4^- stabilizes the colloid for long durations. As previously stated, such nanoparticles can be considered ligand-free from the standpoint of 4-NP reduction because the $NaBH_4$ used in their synthesis is already present in high excess (100×) during the catalytic reduction of 4-NP. Together these two syntheses provide a colloidal platform that is, in many ways, equivalent to the substrate-based platform used to assess ligand desorption but with the advantage that the amount of catalyst added to a reaction can be significantly increased over what is practicable for substrate-based structures. Figure 3 shows transmission electron microscopy (TEM) images, histograms of the nanoparticle diameters, and optical characterization for the Au colloids produced. The BH_4^--based synthesis yields near-spherical nanoparticles with an average diameter of 5.8 nm that exhibit a plasmon resonance at 515 nm. The citrate-based synthesis yields similarly shaped structures with a larger average diameter of 13.4 nm and a correspondingly higher LSPR value of 519 nm. When the citrate ligand is exchanged for PVP and 4-ATP, the plasmon resonance red shifts to 523 and 528 nm, respectively.

The Au catalysts with three different ligands as well as the ligand-free nanoparticles were evaluated for their ability to drive 4-NP reduction. For each experiment, the catalyst of interest was injected into a 2.5 cm path length cuvette to a form a 12.5 mL solution of 50 μM 4-NP and 20 mM $NaBH_4$. The cuvette, which is larger than what is typically used in 4-NP reduction experiments, facilitates the insertion of a probe that provides for real time monitoring of the dissolved oxygen content within the aqueous reactants while simultaneously monitoring the time-dependent spectroscopic signal resulting from the 400 nm 4-NP absorbance. Catalysts were assessed in reactants that were purged with Ar gas to rid them of dissolved oxygen and in unpurged reactants initially containing dissolved

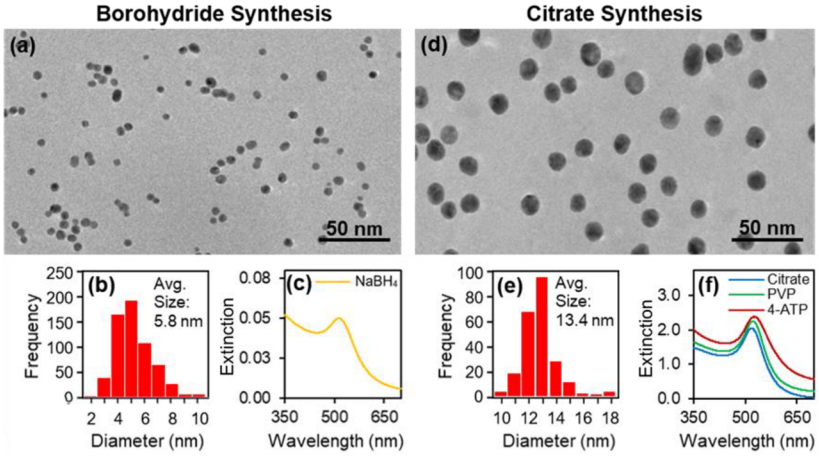

Figure 3. TEM images of colloidal nanoparticles, their size distribution, and extinction spectra for (a−c) borohydride- and (d−f) citrate-based syntheses. The extinction spectra labeled PVP and 4-ATP in (f) correspond to citrate-based nanoparticles that subsequently underwent a ligand exchange process.

https://dx.doi.org/10.1021/acscatal.0c02759
ACS Catal. 2020, 10, 10040−10050

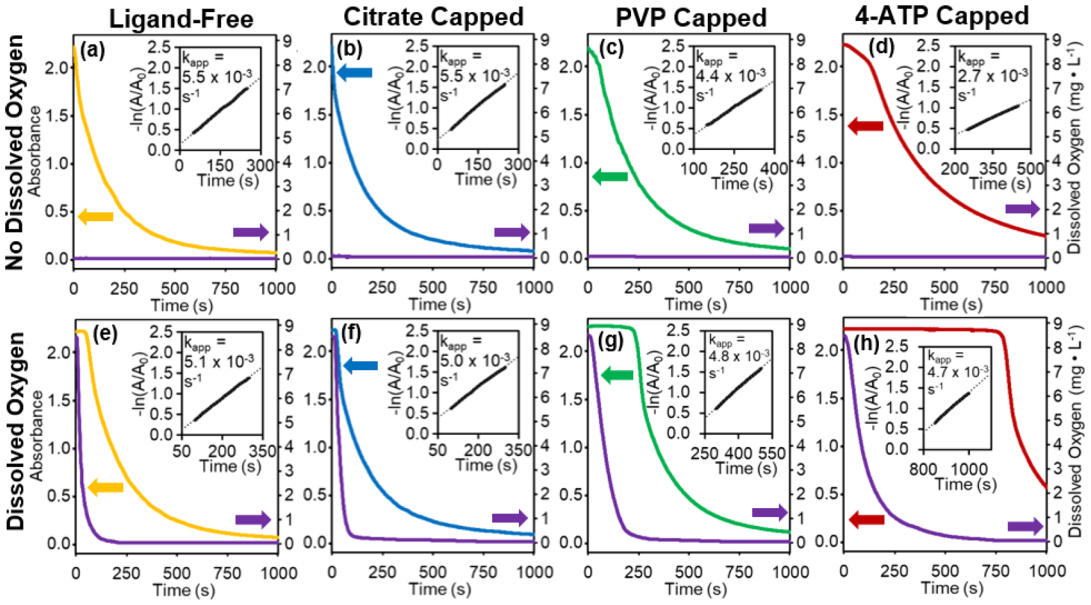

Figure 4. Catalysis data showing the time-dependent 4-NP absorbance alongside the time-dependent concentration of dissolved oxygen within the aqueous reactants for Au catalysts that are (a, e) ligand-free and to which (b, f) citrate, (c, g) PVP, and (d, h) 4-ATP ligands are adsorbed. The data on the top row utilized reactants that were purged of dissolved oxygen, while the bottom row used reactants with dissolved oxygen.

oxygen at the ambient value concentration (i.e., 8.3 mg·L^{-1}). Details regarding the experimental setup are described elsewhere.[29]

Figure 4 shows the time-dependence of both the 4-NP absorbance and the dissolved oxygen concentration for all four Au catalysts for scenarios where the dissolved oxygen is removed (i) prior to the reaction using an Ar gas purge (Figure 4a–d) and (ii) during the reaction through BH_4^- oxidation where the product is boric acid (H_3BO_3).[70] The insets to each graph show a–ln(A/A_0) versus time plot and lists the k_{app} value extracted from it. In the absence of dissolved oxygen, the ligand-free absorbance data (Figure 4a) shows (i) no induction time, (ii) follows pseudo-first-order reaction kinetics, and (iii) yields a k_{app} value that is in line with prior studies.[54,59] In the presence of dissolved oxygen (Figure 4e), the data shows (i) a dissolved oxygen content that precipitously falls, (ii) an induction time of 50 s that abruptly ends once the dissolved oxygen content has been diminished to near-zero values, and (iii) a k_{app} value that is slightly lower than the one obtained when the dissolved oxygen is purged. For the latter case, the lower value is due to residual levels of dissolved oxygen that fuel a side reaction that acts in opposition to 4-NP reduction.[29−31] The ligand-free data is, hence, exactly as expected for bare catalysts and confirms that the BH_4^--derived colloidal nanoparticles act as an effective control for comparing their response to that of ligand-capped catalysts. There is, however, the caveat that these nanoparticles are somewhat smaller in diameter than those used in all other measurements (Figure 3), and as such, they present a larger surface-area for catalysis if the same amount of Au is used. In an effort to compensate for this discrepancy, the amount of ligand-free catalyst added was tuned to give a k_{app} value similar to that obtained for all three ligand-coated samples for the scenario where dissolved oxygen is present in the reactants (Figure 4f–h), the logic being that the k_{app} value is nearly independent of the ligand for this scenario because, in all cases, they have been removed during the induction period (vide infra).

When the citrate-, PVP-, and 4-ATP-capped catalysts are introduced into reactants free of dissolved oxygen (Figure 4b–d), the absorbance immediately begins to decline but where the PVP and 4-ATP results show a characteristic kink after which the rate of reaction increases significantly. With the time span required for the desorption of these two ligands (Figure 1) being commensurate with the time by which the kink occurs, this period of lessened catalytic activity is attributed to the inaccessibility of active sites on the Au nanoparticle due to ligand attachment. Once the ligands desorb from these sites, the reaction proceeds at the faster rate that occurs beyond the kink feature. The kink itself could originate from ligand desorption from the low coordination sites present on roundish Au surfaces[71] since such ligands are likely to be more strongly bound to these sites but, once removed, expose low coordination Au sites that lead to higher catalytic activity. Consistent with the explanation is that the citrate ligand, which desorbs most rapidly from Au, does not give rise to a kink feature. The results are revealing in that they show that the PVP- and 4-ATP-capped catalyst can, in the absence of dissolved oxygen, exhibit an induction-time-like feature. This ligand-induced induction period is, however, distinct in that it is characterized by a gradual, rather than sudden, "turning on" of the reaction. The data also suggests that ligands remain detrimental to catalysis even beyond the kink feature, with the most strongly bonded ligand (i.e., 4-ATP) being most effected in that it shows a k_{app} value that is half that of the most weekly bonded ligand (i.e., citrate).

When the citrate-, PVP-, and 4-ATP-capped catalysts are introduced into reactants with dissolved oxygen (Figure 4f–h), they all exhibit an induction period that ends with the sudden onset of catalytic turnover. The duration of the induction period trends with the bonding strength of the ligand to the Au catalyst but where the time span required for the citrate-capped catalysts is unexpectedly small (<30 s). Although such results could be interpreted as ligands being responsible for the induction time, the time dependence of the dissolved oxygen content within the reactants suggests that the ligand influence

https://dx.doi.org/10.1021/acscatal.0c02759
ACS Catal. 2020, 10, 10040−10050

is indirect. This data, in agreement with prior work, shows that the induction time ends only after the dissolved oxygen has been consumed,[29] but where the rate of consumption depends on the ligand type. These rates, as obtained using first-order reaction kinetics, are reported in Figure S5. To understand the mechanism by which this indirect ligand effect occurs, it must first be recognized that the consumption of dissolved oxygen is dramatically sped up by the catalyst.[30] Therefore, it follows that a slower rate of ligand desorption will lead to the slower removal of dissolved oxygen because less catalytically active sites are available. It should also be noted that the ligand-induced kink feature observed when dissolved oxygen is removed prior to the onset the reaction (Figure 4c, d) is absent in this data because the time scale of the dissolved-oxygen-induced induction period is much longer, and as such, the ligand removal occurs before the induction period has ended. In such a scenario, it is anticipated that each of the three ligand-capped Au catalysts exit the induction period more or less identical since most of the ligands have been removed, an outcome that is confirmed by k_{app} values that differ by no more than 6% (Figure 4f–h). The implication of this result is that the intrinsic catalytic activity of a nanostructure is more accurately benchmarked in reactants that initially contain dissolved oxygen, a result that is contradiction to best practices.

With the citrate-capped Au nanoparticles showing an unexpectedly brief induction time when introduced into reactants containing dissolved oxygen (Figure 4f), as well as a time-dependent dissolved oxygen content that fell faster than it did for the ligand-free structures, experiments were carried out to determine if the presence of citrate contributed to the consumption of dissolved oxygen. Figure 5 shows the results of

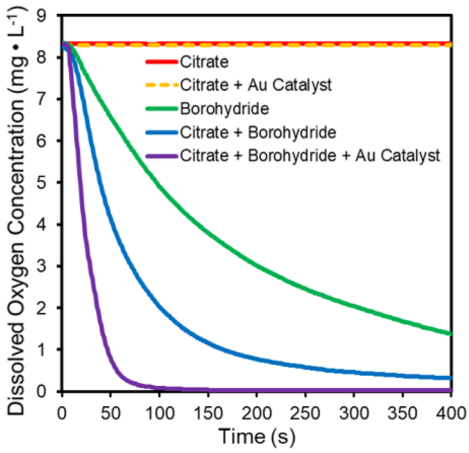

Figure 5. Time dependence of the dissolved oxygen content for an aqueous solution to which various combinations of chemicals and catalysts are added. The concentrations of citrate, borohydride, and citrate capped Au catalyst used to obtain these results are 34 mM, 20 mM, and 4.6 μM, respectively.

a series of tests where various chemicals and Au catalysts were added to water while monitoring the dissolved oxygen content in real time. The data shows that neither citrate nor Au catalysts plus citrate alter the dissolved oxygen content on time scales of relevance to the observed induction time. Adding citrate in tandem with BH_4^-, however, results in a rate of decline in the dissolved oxygen content that exceeds that when just BH_4^- is added. When Au nanoparticles are added in addition to citrate and $NaBH_4$, the reaction is sped up further, a result that shows that the reaction leading to oxygen consumption can be catalytically enhanced. Figure S6 presents additional results that show that the rate of the dissolved oxygen consumption reaction is sped up even further when more Au catalyst is added. Data showing that no equivalent enhancement effect exists for PVP and 4-ATP are also presented in Figure S7. Together, this data not only accounts for the unusually brief induction time for the citrate-capped catalyst but, in a broader sense, demonstrates that the idiosyncrasies of individual capping agents can materially alter 4-NP reduction.

DISCUSSION

The catalytic reduction of 4-NP is a reaction where seemingly innocuous parameters and unexpected interdependencies can assert control over the reaction. Ligand desorption from colloidal catalysts, in many ways, exemplifies this point in that a comprehensive understanding can only be attained if the nuances of this process are understood. Although contradictory conclusions regarding the influence of ligands appear in the literature, many of them can be rationalized through the understanding gained in the current study. It has, for example, been repeatedly argued that ligands are responsible for the induction time despite convincing evidence showing that its origins stem from the presence of dissolved oxygen. With the understanding that ligands temporarily block catalytic sites that would otherwise speed up the consumption of dissolved oxygen, it is possible to explain results showing the addition of progressively more ligands to the catalyst surface leads to a lengthening of the induction time. The fact that citrate can lead to the rapid removal of dissolved oxygen also accounts for the fact that citrate-based nanoparticle syntheses show negligible induction times.[5] In addition to this indirect influence, the current study also shows that an induction-time-like feature can appear when oxygen-free reactants are used to benchmark catalysts with strongly bound ligands. This ligand-induced induction period is, however, distinct in that the reaction gradually "turns on" before a rapid increase that is characterized by kink in the time-dependent absorbance. This finding accounts for another subset of results from past studies. Likewise, reports in the literature claiming that ligands have little influence on k_{app} values are understood if the ligand is weakly bound or if a dissolved-oxygen-induced induction time of sufficient length provides the time needed for the ligands to desorb prior to the onset of the reaction. Additionally, reports concluding that ligands have a decisive impact on k_{app} can be rationalized if the dissolved oxygen was purged from the reactants before the addition of the ligand-capped catalysts. The removal of ligands by BH_4^- also contributes to the different k_{app} values obtained when the reactant mixing sequence is varied[5] because it leads to different BH_4^- exposure times. It should also be noted that other factors that are known to influence 4-NP reduction, such as pH[72] and BH_4^- concentration,[30] are also likely to impact the ligand removal process.

With the current findings in support of a literature that labels BH_4^- as a "general purpose detergent" for the removal of ligands from colloidal nanostructures, it is highly likely that such effects are commonplace. It should, nonetheless, be recognized that not every ligand is removed by BH_4^- as examples do exist where 4-NP reduction is severely impeded by the attachment of ligands (Figure S8).[4] The understanding gained raises significant concerns but also provides oppor-

https://dx.doi.org/10.1021/acscatal.0c02759
ACS Catal. 2020, 10, 10040−10050

tunities. The ability to remove capping ligands from nanostructure surfaces using BH_4^- leaves them more catalytically active than they would otherwise be. If a ligand-capped catalyst is immobilized on a retrievable support, then it will be free of ligands upon first retrieval. Negative impacts, however, can result in that some ligands, such as CTAB, are cytotoxic, and as such, their loss to liquid media can lead to the release of harmful pollutants. Moreover, any protection afforded to the nanostructure by the ligand that would otherwise lead to a longer lifespan is lost. From this standpoint catalyst leaching is a particular concern, especially if the reactants contain dissolved oxygen since oxidative etching is the primary driver for this process. Although such concerns are minimal for Au catalysts, other leach-prone nanostructures, such as Ag and Cu, are highly susceptible.[32,34] Scenarios can even develop where the catalyst, once it has lost its ligands, loses much of its catalytic activity due to leaching or where leached material gives rise to the formation of smaller nanostructures that become a new catalytic entity that is far more active.[32] In certain instances, it could, therefore, prove advantageous to reapply the ligand upon retrieval to regain this protection.

On the basis of the understanding derived from this study, recommendations can be made on the use of 4-NP as a model catalytic reaction. The purging of all aqueous solutions used in 4-NP reduction with an inert gas prior to usage is widely practiced as a means to rid the results of the confounding influences of dissolved oxygen; however, for ligand-capped catalysts this practice can lead to diminished k_{app} values that are not representative of the intrinsic catalytic activity of the nanostructure under investigation. Alternatively, if reactants containing dissolved oxygen are used, then the catalyst under study is susceptible to leaching or somewhat diminished k_{app} values resulting from residual levels of dissolved oxygen. A best practice procedure is, hence, forwarded in which the catalyst under study is pretreated with BH_4^- that has been purged with an inert gas. In this manner, the catalyst will enter the reaction without ligands and where its ligand-free surface has never been exposed to dissolved oxygen. A pretreatment of significant duration also lessens the concern that ligand effects may be more acute when using elements or alloys where the ligand−metal bond strength is greater than it is for Au. Additionally, high catalyst loading should be avoided to limit any adverse effects that could arise due to the readsorption of ligands within the aqueous media. When such practices are used, it should be recognized that 4-NP reduction becomes a measure of the intrinsic catalytic activity of the ligand-free nanostructure, a result that is contrary to the prevailing sentiment where it is assumed that it is the ligand-capped structure that is being probed. A demonstration validating the effectiveness of the proposed procedure is presented in Figure S9.

CONCLUSION

The results presented in this study show that ligands have a pronounced influence upon 4-NP reduction that is largely due to the propensity that BH_4^- has for displacing ligands on catalytic surfaces where the exact impact is dependent on whether dissolved oxygen is present in the aqueous reactants. By showing that strongly bound ligands give rise to an induction-time-like feature in the time-dependent absorbance for reactants that are free of dissolved oxygen while exhibiting no such feature when dissolved oxygen is present, the work adds clarity to the longstanding controversy as to whether ligands are responsible for the induction time. The study also indicates that the intrinsic k_{app} value of nanostructures is most accurately benchmarked if the structures are exposed to BH_4^- prior to the onset of the reaction because it provides the time needed for ligand removal. Alternatively, if the goal is to examine ligand influences on 4-NP reduction then they are most readily observed when all reactants are purged of dissolved oxygen. Together, these findings advance the mechanistic framework governing the catalytic reduction of 4-NP, provide recommendations for the accurate benchmarking of catalytic activity, and further emphasizes the importance of ligand−nanoparticle interrelationships in determining catalytic behavior.

EXPERIMENTAL SECTION

Chemicals and Materials. Au films were deposited on two-side polished 10 mm × 10.5 mm × 0.6 mm [0001]-oriented sapphire substrates (MTI Corp.) using a sputter target cut from a 0.5 mm thick Au foil (99.9985% purity, Alfa Aesar) and dewetted in ultrahigh purity Ar (Airgas). The synthesis of Au colloids used tetrachloroaurate (III) trihydrate ($HAuCl_4 \cdot 3H_2O$, MilliporeSigma). Sodium citrate ($Na_3C_6H_5O_7$), polyvinylpyrrolidone (PVP, average mol. wt. 40,000), and 4-aminothiophenol (4-ATP) were sourced from Alfa Aesar, MilliporeSigma, and VWR, respectively. Catalysis and ligand desorption experiments utilized 4-nitrophenol (4-NP, Fluka) and sodium borohydride ($NaBH_4$, MilliporeSigma). All aqueous solutions were prepared using deionized (DI) water derived from a Milli-Q system (18.2 MΩ·cm at 25 °C).

Nanostructure Preparation. *Substrate-Immobilized Au Nanostructures.* Ultrathin films of Au were sputter deposited to a thickness of 2.1 nm using a Gatan Model 681 High Resolution Ion Beam Coater. Films were then exposed to a heating regimen in an Ar-purged Thermo Scientific Lindberg Blue M tube furnace that sees the temperature ramped to 900 °C over a 45 min period followed by ambient cooling to room temperature. When required, ligands were applied to the Au nanostructures immediately after their removal from the furnace by submerging them in concentrated solutions of the capping ligand and allowing them to incubate for 30 min. Citrate and PVP capping utilized aqueous solutions with molarities of 10 and 1 mM, respectively, while 4-ATP capping utilized a molarity of 30 mM in combination with an ethanol solvent. For all cases, samples were rinsed in ethanol to remove excess capping agent from the exposed substrate surface. Once prepared, the ligand-coated samples were immediately subjected to the desired characterization procedure.

Borohydride-Based Au Nanoparticle Synthesis. Colloidal Au nanoparticles stabilized by sodium BH_4^- were prepared using a method similar to that described by Deraedt et al.[59] in which Au^{3+} ions are reduced by BH_4^- in an aqueous solution of $HAuCl_4$ and $NaBH_4$. The room temperature procedure begins by first preparing a stock solution of DI water that is purged with Ar gas for 15 min to remove the dissolved oxygen. Aqueous $NaBH_4$ (9 mL, 13 mM) is then prepared where minimal agitation is used to dissolve the powder so as to limit the uptake of dissolved oxygen. Once fully dissolved, 1 mL of the solution was added to 9 mL of aqueous $HAuCl_4$ (144 μM), which also underwent a 15 min Ar gas purge, to create a 130 μM solution of Au nanoparticles. The reaction resulted in an immediate color change from clear to purple. The resulting colloid was then purged with Ar gas for an additional 5 min and left to sit overnight in the dark.

https://dx.doi.org/10.1021/acscatal.0c02759
ACS Catal. 2020, 10, 10040−10050

Citrate-Based Au Nanoparticle Synthesis. Citrate-stabilized colloidal Au nanoparticles were synthesized using the Turkevich method.[68,69] $HAuCl_4$ (0.125 mmol) was dissolved in 220 mL of DI water and brought to a boil under constant stirring. Sodium citrate (12.5 mL, 34 mM) was then rapidly added and vigorously boiled under continued stirring for 30 min, a process that caused a slow color change from near-transparent to a deep red hue. The synthesis ended with ambient cooling followed by overnight storage in the dark. The final solution had an Au concentration of 0.57 mM.

Ligand Exchange Processes. Colloidal Au nanoparticles capped with PVP and 4-ATP were prepared using ligand exchange processes. The citrate-for-PVP exchange utilized the method reported by Graf et al.[73] in which powdered PVP (MW 40 000, 0.4 g) was added to colloidal Au nanoparticles (10 mL, 0.57 mM) prepared using the aforementioned citrate-based synthesis. The ligand exchange proceeded overnight under gentle magnetic stirring in the dark. The PVP-for-4-ATP exchange utilized a method similar to that reported by Moran et al.[74] in which 4-ATP (0.1 mL, 10 mM) is added to PVP-capped Au nanoparticles (10 mL, 0.57 mM). This ligand exchange also occurred overnight in the dark under gentle stirring. It should be noted that a citrate-for-4-ATP exchange proves unsatisfactory due to nanoparticle agglomeration.

Time-Dependent Ligand Desorption Measurements. Substrate-immobilized Au nanostructures with various capping agents were clipped to a 3D-printed plastic sample holder that, when placed over a cuvette, positions the sample in the optical path of a Jasco V-730 Spectrophotometer. The setup required that the spectrometer sample compartment be retrofitted to accommodate the custom-built 2.5 cm path-length borosilicate cuvettes (Specialty Glass Products) required.[29] Optical characterization proceeded after submerging the sample in 10.5 mL of DI water and then rapidly adding aqueous $NaBH_4$ (2 mL, 125 mM) to achieve a final molarity of 20 mM. Successive absorbance spectra were taken approximately every 60 s for the 900 s duration of the experiment. All spectra were baselined using a sapphire substrate submerged in DI water.

4-NP Catalysis. All spectroscopic monitoring of 4-NP catalysis was carried out using the previously described instrumentation but where a Vernier Optical Dissolved Oxygen Probe was inserted into the cuvette to allow for real time monitoring of the dissolved oxygen content within the reactants. Once the probe was inserted, the cuvette was sealed with Parafilm held in place by a Viton O-ring. A Teflon tube was inserted into the Parafilm to allow Ar gas to be gently flowed over the reactant surface after which it exhausts through a small pinhole. This purging procedure was carried out regardless of whether the aqueous reactants were purged to prevent the additional uptake of dissolved into the aqueous solution. All catalytic reactions were carried out in 12.5 mL of aqueous 4-NP (50 μM) and $NaBH_4$ (20 mM). Ligand-capped and ligand-free colloidal catalysts were added at Au concentrations of 4.6 and 0.8 μM, respectively. All spectroscopic measurements monitored the 400 nm 4-NP peak absorbance wavelength. It should be noted that the Au catalyst has negligible absorbance for the concentrations used. Reactions carried out in the absence of dissolved oxygen saw the 4-NP and catalyst solutions each purged with Ar gas for 15 min. The $NaBH_4$ solution was prepared by purging the water of dissolved oxygen and then adding the $NaBH_4$ powder to it. Upon mixing the $NaBH_4$, the cuvette was immediately filled with the various solutions in the order (i) 4-NP, (ii) $NaBH_4$, and (iii) Au catalyst where the timing for all procedures was kept as constant as possible to promote reproducibility. Reactions carried out with dissolved oxygen proceeded in a similar manner but where the 4-NP and Au solutions, as well as the water used for $NaBH_4$, were exposed to open air for 2 h to allow the time needed for the dissolved oxygen content to equilibrate. For a typical experiment, the starting and ending pH values as measured by a HM Digital PH-200 pH Meter are 10.1 and 10.4, respectively. Each catalysis experiment was carried out five times and plotted as an average.

Catalyst Characterization. *Electron Microscopy.* Substrate-immobilized Au nanoparticles were imaged using a Magellan 400 FEI Field Emission Scanning Electron Microscope (FESEM) using a secondary electron detector operating in immersion mode. Colloidal Au nanoparticles were drop-cast onto TEM grids with an ultrathin carbon film supported by a lacey carbon film on 400 mesh copper (Ted Pella) and imaged with a JEOL 2011 Transmission Electron Microscope.

XPS Detection of 4-ATP Removal by $NaBH_4$. Two identical samples of substrate-immobilized Au nanoparticles were prepared and then incubated in 4-ATP solution using the aforementioned procedures. One sample was left in this state while the other sample was exposed to aqueous $NaBH_4$ (12.5 mL, 20 mM) for 15 min after which it was removed and rinsed in ethanol. Both samples were then scanned using XPS. Photoelectron spectra were collected using an Ambient Pressure X-ray Photoelectron Spectrometer (AP-XPS) manufactured by SPECS Surface Nano Analysis GmbH, Germany. Measurements were carried out at a base pressure of approximately 5×10^{-10} mbar where a monochromatic Al K_α X-ray beam with a photon energy of 1486.6 eV was used to produce photoelectrons. The spectra obtained for each sample was calibrated by adjusting the binding energy position of Au $4f_{7/2}$ peak to 84 eV.

Time Dependence of the Dissolved Oxygen Concentration. The dissolved oxygen measurements during 4-NP catalysis were obtained using a Vernier Optical Dissolved Oxygen Probe submerged in the reaction solution. The oxygen probe was inserted into a cuvette that was sealed with Parafilm. An Ar gas purge line was inserted through the Parafilm to lightly blow Ar over the top surface of the reactants to prevent the uptake of dissolved oxygen where a small pinhole acted as an exhaust. Dissolved oxygen monitoring was performed in separate experiments from 4-NP monitoring, where the reaction conditions for each experiment were kept identical and oxygen monitoring was initiated immediately after the ligand-capped or ligand-free colloidal catalyst of interest was added to the reaction solution. Measurements for monitoring the time dependence of dissolved oxygen removal as a function of citrate and the amount of added catalyst were obtained in a similar manner. For all cases, there exists a brief interval at the beginning of the reaction where oxygen removal appears suppressed but which is actually associated with the response time of the sensor and the time needed for the injected chemicals to form a mixture.

■ ASSOCIATED CONTENT

Supporting Information

The Supporting Information is available free of charge at https://pubs.acs.org/doi/10.1021/acscatal.0c02759.

Additional information is provided in the form of (i) further characterization of the substrate-supported

https://dx.doi.org/10.1021/acscatal.0c02759
ACS Catal. 2020, 10, 10040−10050

catalysts, (ii) optical and spectroscopic characterization of the ligand and ligand-free catalysts, (iii) an analysis of the kinetics of ligand desorption and dissolved oxygen consumption, (iv) additional monitoring of the rate at which dissolved oxygen is removed by $NaBH_4$ in the presence of citrate with varying amounts of catalyst, (v) measurements confirming that PVP and 4-ATP ligands do not alter the dissolved oxygen content, (vi) data showing that certain ligands exist that remain attached to the catalysts when exposed to borohydride, (vii) data validating a new procedure for benchmarking catalysts using 4-NP reduction, and (viii) tables listing the standard deviations for the k_{app} values reported (PDF)

AUTHOR INFORMATION

Corresponding Author

Svetlana Neretina − *College of Engineering and Department of Chemistry & Biochemistry, University of Notre Dame, Notre Dame, Indiana 46556, United States;* orcid.org/0000-0002-6889-4384; Email: sneretina@nd.edu

Authors

Robert D. Neal − *College of Engineering, University of Notre Dame, Notre Dame, Indiana 46556, United States*

Robert A. Hughes − *College of Engineering, University of Notre Dame, Notre Dame, Indiana 46556, United States*

Pitambar Sapkota − *Department of Physics and Notre Dame Radiation Laboratory, University of Notre Dame, Notre Dame, Indiana 46556, Unites States*

Sylwia Ptasinska − *Department of Physics and Notre Dame Radiation Laboratory, University of Notre Dame, Notre Dame, Indiana 46556, Unites States;* orcid.org/0000-0002-7550-8189

Complete contact information is available at: https://pubs.acs.org/10.1021/acscatal.0c02759

Author Contributions

The manuscript was written through contributions of all authors. All authors have given approval to the final version of the manuscript.

Funding

This work is supported by National Science Foundation Award (DMR-1803917) to S.N. P.S. and S.P. are supported by the US Department of Energy Office of Science, Office of Basic Energy Sciences under Award Number DE-FC02-04ER15533 (NDRL# 5291).

Notes

The authors declare no competing financial interest.

ACKNOWLEDGMENTS

The authors have benefited from the facilities available through the Notre Dame Integrated Imaging Facility (NDIIF). The authors wish to acknowledge the technical expertise provided by Maksym Zhukovskyi in carrying out the TEM work. R.D.N. wishes to acknowledge A. Katzelis (Mishawaka High School) for assistance with laboratory work.

REFERENCES

(1) Lee, H.; Yoon, D. E.; Koh, S.; Kang, M. S.; Lim, J.; Lee, D. C. Ligands as a Universal Molecular Toolkit in Synthesis and Assembly of Semiconductor Nanocrystals. *Chem. Sci.* **2020**, *11*, 2318−2329.

(2) Yang, T.-H.; Shi, Y.; Janssen, A.; Xia, Y. Surface Capping Agents and Their Roles in Shape-Controlled Synthesis of Colloidal Metal Nanocrystals. *Angew. Chem., Int. Ed.* **2020**, DOI: 10.1002/anie.201911135.

(3) Ortiz, N.; Skrabalak, S. E. On the Dual Roles of Ligands in the Synthesis of Colloidal Metal Nanostructures. *Langmuir* **2014**, *30*, 6649−6659.

(4) Ansar, S. M.; Kitchens, C. L. Impact of Gold Nanoparticle Stabilizing Ligands on the Colloidal Catalytic Reduction of 4-Nitrophenol. *ACS Catal.* **2016**, *6*, 5553−5560.

(5) Álvarez Cerimedo, M. S.; Baronio, L. G.; Hoppe, C. E.; Ayude, M. A. The Effect of Poly(Vinylpyrrolidone) (PVP) on the Au Catalyzed Reduction of p-Nitrophenol: The Fundamental Role of $NaBH_4$. *ChemistrySelect* **2019**, *4*, 608−616.

(6) Gao, M.; Yang, Y.; Guo, J. Revealing the Role of Chain Length of Ligands on Gold Nanoparticles Surface in the Process for Catalysis Reduction of 4-Nitrophenol. *Catal. Lett.* **2019**, *149*, 2110−2118.

(7) Lopez-Sanchez, J. A.; Dimitratos, N.; Hammond, C.; Brett, G. L.; Kesavan, L.; White, S.; Miedziak, P.; Tiruvalam, R.; Jenkins, R. L.; Carley, A. F.; Knight, D.; Kiely, C. J.; Hutchings, G. J. Facile Removal of Stabilizer-Ligands from Supported Gold Nanoparticles. *Nat. Chem.* **2011**, *3*, 551−556.

(8) Rossi, L. M.; Fiorio, J. L.; Garcia, M. A. S.; Ferraz, C. P. The Role and Fate of Capping Ligands in Colloidally Prepared Metal Nanoparticle Catalysts. *Dalt. Trans.* **2018**, *47*, 5889−5915.

(9) Liu, Y.; Jia, C. N.; Yamasaki, J.; Terasaki, O.; Schüth, F. Highly Active Iron Oxide Supported Gold Catalysts for CO Oxidation: How Small Must the Gold Nanoparticles Be? *Angew. Chem., Int. Ed.* **2010**, *49*, 5771−5775.

(10) Campisi, S.; Schiavoni, M.; Chan-Thaw, C. E.; Villa, A. Untangling the Role of the Capping Agent in Nanocatalysis: Recent Advances and Perspectives. *Catalysts* **2016**, *6*, 185.

(11) Bastús, N. G.; Merkoçi, F.; Piella, J.; Puntes, V. Synthesis of Highly Monodisperse Citrate-Stabilized Silver Nanoparticles of up to 200 nm: Kinetic Control and Catalytic Properties. *Chem. Mater.* **2014**, *26*, 2836−2846.

(12) Niu, Z.; Li, Y. Removal and Utilization of Capping Agents in Nanocatalysis. *Chem. Mater.* **2014**, *26*, 72−83.

(13) Park, J. Y.; Aliaga, C.; Renzas, J. R.; Lee, H.; Somorjai, G. A. The Role of Organic Capping Layers of Platinum Nanoparticles in Catalytic Activity of CO Oxidation. *Catal. Lett.* **2009**, *129*, 1−6.

(14) Wang, Z.; Fu, H.; Han, D.; Gu, F. The Effects of Au Species and Surfactant on the Catalytic Reduction of 4-Nitrophenol by Au@SiO_2. *J. Mater. Chem. A* **2014**, *2*, 20374−20381.

(15) Ibrahim, M.; Garcia, M. A. S.; Vono, L. L. R.; Guerrero, M.; Lecante, P.; Rossi, L. M.; Philippot, K. Polymer: Versus Phosphine Stabilized Rh Nanoparticles as Components of Supported Catalysts: Implication in the Hydrogenation of Cyclohexene Model Molecule. *Dalt. Trans.* **2016**, *45*, 17782−17791.

(16) Schrader, I.; Warneke, J.; Backenköhler, J.; Kunz, S. Functionalization of Platinum Nanoparticles with L-Proline: Simultaneous Enhancements of Catalytic Activity and Selectivity. *J. Am. Chem. Soc.* **2015**, *137*, 905−912.

(17) Wang, Y.; Wan, X. K.; Ren, L.; Su, H.; Li, G.; Malola, S.; Lin, S.; Tang, Z.; Häkkinen, H.; Teo, B. K.; Wang, Q. M.; Zheng, N. Atomically Precise Alkynyl-Protected Metal Nanoclusters as a Model Catalyst: Observation of Promoting Effect of Surface Ligands on Catalysis by Metal Nanoparticles. *J. Am. Chem. Soc.* **2016**, *138*, 3278−3281.

(18) Yoskamtorn, T.; Yamazoe, S.; Takahata, R.; Nishigaki, J. I.; Thivasasith, A.; Limtrakul, J.; Tsukuda, T. Thiolate-Mediated Selectivity Control in Aerobic Alcohol Oxidation by Porous Carbon-Supported Au_{25} Clusters. *ACS Catal.* **2014**, *4*, 3696−3700.

(19) Li, G.; Qian, H.; Jin, R. Gold Nanocluster-Catalyzed Selective Oxidation of Sulfide to Sulfoxide. *Nanoscale* **2012**, *4*, 6714−6717.

(20) Hervés, P.; Pérez-Lorenzo, M.; Liz-Marzán, L. M.; Dzubiella, J.; Lu, Y.; Ballauff, M. Catalysis by Metallic Nanoparticles in Aqueous Solution: Model Reactions. *Chem. Soc. Rev.* **2012**, *41*, 5577−5587.

(21) Zhao, P.; Feng, X.; Huang, D.; Yang, G.; Astruc, D. Basic Concepts and Recent Advances in Nitrophenol Reduction by Gold- and Other Transition Metal Nanoparticles. *Coord. Chem. Rev.* **2015**, *287*, 114−136.
(22) Aditya, T.; Pal, A.; Pal, T. Nitroarene Reduction: A Trusted Model Reaction to Test Nanoparticle Catalysts. *Chem. Commun.* **2015**, *51*, 9410−9431.
(23) Wunder, S.; Polzer, F.; Lu, Y.; Mei, Y.; Ballauff, M. Kinetic Analysis of Catalytic Reduction of 4-Nitrophenol by Metallic Nanoparticles Immobilized in Spherical Polyelectrolyte Brushes. *J. Phys. Chem. C* **2010**, *114*, 8814−8820.
(24) Wunder, S.; Lu, Y.; Albrecht, M.; Ballauff, M. Catalytic Activity of Faceted Gold Nanoparticles Studied by a Model Reaction: Evidence for Substrate-Induced Surface Restructuring. *ACS Catal.* **2011**, *1*, 908−916.
(25) Antonels, N. C.; Meijboom, R. Preparation of Well-Defined Dendrimer Encapsulated Ruthenium Nanoparticles and Their Evaluation in the Reduction of 4-Nitrophenol According to the Langmuir-Hinshelwood Approach. *Langmuir* **2013**, *29*, 13433−13442.
(26) Suchomel, P.; Kvitek, L.; Prucek, R.; Panacek, A.; Halder, A.; Vajda, S.; Zboril, R. Simple Size-Controlled Synthesis of Au Nanoparticles and Their Size-Dependent Catalytic Activity. *Sci. Rep.* **2018**, *8*, 4589.
(27) Panáček, A.; Prucek, R.; Hrbáč, J.; Nevečná, T.; Šteffková, J.; Zbořil, R.; Kvítek, L. Polyacrylate-Assisted Size Control of Silver Nanoparticles and Their Catalytic Activity. *Chem. Mater.* **2014**, *26*, 1332−1339.
(28) Khalavka, Y.; Becker, J.; Sönnichsen, C. Synthesis of Rod-Shaped Gold Nanorattles with Improved Plasmon Sensitivity and Catalytic Activity. *J. Am. Chem. Soc.* **2009**, *131*, 1871−1875.
(29) Menumerov, E.; Hughes, R. A.; Neretina, S. Catalytic Reduction of 4-Nitrophenol: A Quantitative Assessment of the Role of Dissolved Oxygen in Determining the Induction Time. *Nano Lett.* **2016**, *16*, 7791−7797.
(30) Neal, R. D.; Inoue, Y.; Hughes, R. A.; Neretina, S. Catalytic Reduction of 4-Nitrophenol by Gold Catalysts: The Influence of Borohydride Concentration on the Induction Time. *J. Phys. Chem. C* **2019**, *123*, 12894−12901.
(31) Strachan, J.; Barnett, C.; Masters, A. F.; Maschmeyer, T. 4-Nitrophenol Reduction: Probing the Putative Mechanism of the Model Reaction. *ACS Catal.* **2020**, *10*, 5516−5521.
(32) Menumerov, E.; Hughes, R. A.; Golze, S. D.; Neal, R. D.; Demille, T. B.; Campanaro, J. C.; Kotesky, K. C.; Rouvimov, S.; Neretina, S. Identifying the True Catalyst in the Reduction of 4-Nitrophenol: A Case Study Showing the Effect of Leaching and Oxidative Etching Using Ag Catalysts. *ACS Catal.* **2018**, *8*, 8879−8888.
(33) Zhang, Q.; Blom, D. A.; Wang, H. Nanoporosity-Enhanced Catalysis on Subwavelength Au Nanoparticles: A Plasmon-Enhanced Spectroscopic Study. *Chem. Mater.* **2014**, *26*, 5131−5142.
(34) Jenkins, S. V.; Chen, S.; Chen, J. Gold-Copper Alloyed Nanorods for Metal-Catalyzed Organic Reactions: Implication of Surface Ligands on Nanoparticle-Based Heterogeneous Catalysis. *Tetrahedron Lett.* **2015**, *56*, 3368−3372.
(35) Li, J.; Nasaruddin, R. R.; Feng, Y.; Yang, J.; Yan, N.; Xie, J. Tuning the Accessibility and Activity of $Au_{25}(SR)_{18}$ Nanocluster Catalysts through Ligand Engineering. *Chem. - Eur. J.* **2016**, *22*, 14816−14820.
(36) Nasaruddin, R. R.; Chen, T.; Li, J.; Goswami, N.; Zhang, J.; Yan, N.; Xie, J. Ligands Modulate Reaction Pathway in the Hydrogenation of 4-Nitrophenol Catalyzed by Gold Nanoclusters. *ChemCatChem* **2018**, *10*, 395−402.
(37) Nigra, M. M.; Ha, J. M.; Katz, A. Identification of Site Requirements for Reduction of 4-Nitrophenol Using Gold Nanoparticle Catalysts. *Catal. Sci. Technol.* **2013**, *3*, 2976−2983.
(38) Wang, X.; Chen, S.; Reggiano, G.; Thota, S.; Wang, Y.; Kerns, P.; Suib, S. L.; Zhao, J. Au-Cu-M (M = Pt, Pd, Ag) Nanorods with Enhanced Catalytic Efficiency by Galvanic Replacement Reaction. *Chem. Commun.* **2019**, *55*, 1249−1252.
(39) Liu, W.; Yang, X.; Xie, L. Size-Controlled Gold Nanocolloids on Polymer Microsphere-Stabilizer via Interaction between Functional Groups and Gold Nanocolloids. *J. Colloid Interface Sci.* **2007**, *313*, 494−502.
(40) Yamamoto, H.; Yano, H.; Kouchi, H.; Obora, Y.; Arakawa, R.; Kawasaki, H. N,N-Dimethylformamide-Stabilized Gold Nanoclusters as a Catalyst for the Reduction of 4-Nitrophenol. *Nanoscale* **2012**, *4*, 4148−4154.
(41) Shultz, L. R.; McCullough, B.; Newsome, W. J.; Ali, H.; Shaw, T. E.; Davis, K. O.; Uribe-Romo, F. J.; Baudelet, M.; Jurca, T. A Combined Mechanochemical and Calcination Route to Mixed Cobalt Oxides for the Selective Catalytic Reduction of Nitrophenols. *Molecules* **2020**, *25*, 89.
(42) Ansar, S. M.; Ameer, F. S.; Hu, W.; Zou, S.; Pittman, C. U.; Zhang, D. Removal of Molecular Adsorbates on Gold Nanoparticles Using Sodium Borohydride in Water. *Nano Lett.* **2013**, *13*, 1226−1229.
(43) Donoeva, B.; De Jongh, P. E. Colloidal Au Catalyst Preparation: Selective Removal of Polyvinylpyrrolidone from Active Au Sites. *ChemCatChem* **2018**, *10*, 989−997.
(44) Zhang, X.; Liu, B.; Hu, C.; Chen, S.; Liu, X.; Liu, J.; Chen, F.; Chen, J.; Xie, F. A Facile Method in Removal of PVP Ligands from Silver Nanowires for High Performance and Reusable SERS Substrate. *Spectrochim. Acta, Part A* **2020**, *228*, 117733.
(45) Collins, G.; Davitt, F.; O'Dwyer, C.; Holmes, J. D. Comparing Thermal and Chemical Removal of Nanoparticle Stabilizing Ligands: Effect on Catalytic Activity and Stability. *ACS Appl. Nano Mater.* **2018**, *1*, 7129−7138.
(46) Luo, M.; Hong, Y.; Yao, W.; Huang, C.; Xu, Q.; Wu, Q. Facile Removal of Polyvinylpyrrolidone (PVP) Adsorbates from Pt Alloy Nanoparticles. *J. Mater. Chem. A* **2015**, *3*, 2770−2775.
(47) Perera, G. S.; Ansar, S. M.; Hu, S.; Chen, M.; Zou, S.; Pittman, C. U.; Zhang, D. Ligand Desorption and Desulfurization on Silver Nanoparticles Using Sodium Borohydride in Water. *J. Phys. Chem. C* **2014**, *118*, 10509−10518.
(48) Yang, Y.; Wang, Y.; Zhang, X.; Qi, G.; Xu, S.; Xu, W. A Facile Method of Removing Several Common Surface-Enhanced Raman Scattering Probe Molecules Adsorbed on Ag with Sodium Borohydride Solution. *J. Opt.* **2015**, *17*, No. 075003.
(49) Ansar, S. M.; Perera, G. S.; Ameer, F. S.; Zou, S.; Pittman, C. U.; Zhang, D. Desulfurization of Mercaptobenzimidazole and Thioguanine on Gold Nanoparticles Using Sodium Borohydride in Water at Room Temperature. *J. Phys. Chem. C* **2013**, *117*, 13722−13729.
(50) Villarreal, E.; Li, G. G.; Zhang, Q.; Fu, X.; Wang, H. Nanoscale Surface Curvature Effects on Ligand-Nanoparticle Interactions: A Plasmon-Enhanced Spectroscopic Study of Thiolated Ligand Adsorption, Desorption, and Exchange on Gold Nanoparticles. *Nano Lett.* **2017**, *17*, 4443−4452.
(51) Gu, S.; Kaiser, J.; Marzun, G.; Ott, A.; Lu, Y.; Ballauff, M.; Zaccone, A.; Barcikowski, S.; Wagener, P. Ligand-Free Gold Nanoparticles as a Reference Material for Kinetic Modelling of Catalytic Reduction of 4-Nitrophenol. *Catal. Lett.* **2015**, *145*, 1105−1112.
(52) Lebaschi, S.; Hekmati, M.; Veisi, H. Green Synthesis of Palladium Nanoparticles Mediated by Black Tea Leaves (Camellia Sinensis) Extract: Catalytic Activity in the Reduction of 4-Nitrophenol and Suzuki-Miyaura Coupling Reaction under Ligand-Free Conditions. *J. Colloid Interface Sci.* **2017**, *485*, 223−231.
(53) Yamamoto, H.; Yano, H.; Kouchi, H.; Obora, Y.; Arakawa, R.; Kawasaki, H. N,N-Dimethylformamide-Stabilized Gold Nanoclusters as a Catalyst for the Reduction of 4-Nitrophenol. *Nanoscale* **2012**, *4*, 4148−4154.
(54) Menumerov, E.; Hughes, R. A.; Neretina, S. One-Step Catalytic Reduction of 4-Nitrophenol through the Direct Injection of Metal Salts into Oxygen-Depleted Reactants. *Catal. Sci. Technol.* **2017**, *7*, 1460−1464.

https://dx.doi.org/10.1021/acscatal.0c02759
ACS Catal. 2020, 10, 10040−10050

(55) Song, P.; He, L. L.; Wang, A. J.; Mei, L. P.; Zhong, S. X.; Chen, J. R.; Feng, J. J. Surfactant-Free Synthesis of Reduced Graphene Oxide Supported Porous PtAu Alloyed Nanoflowers with Improved Catalytic Activity. *J. Mater. Chem. A* **2015**, *3*, 5321−5327.
(56) Borah, B. J.; Bharali, P. Surfactant-Free Synthesis of CuNi Nanocrystals and Their Application for Catalytic Reduction of 4-Nitrophenol. *J. Mol. Catal. A: Chem.* **2014**, *390*, 29−36.
(57) Miah, A. T.; Bharadwaj, S. K.; Saikia, P. Surfactant Free Synthesis of Gold Nanoparticles within Meso-Channels of Non-Functionalized SBA-15 for Its Promising Catalytic Activity. *Powder Technol.* **2017**, *315*, 147−156.
(58) Zheng, B.; Liu, X.; Wu, Y.; Yan, L.; Du, J.; Dai, J.; Xiong, Q.; Guo, Y.; Xiao, D. Surfactant-Free Gold Nanoparticles: Rapid and Green Synthesis and Their Greatly Improved Catalytic Activities for 4-Nitrophenol Reduction. *Inorg. Chem. Front.* **2017**, *4*, 1268−1272.
(59) Deraedt, C.; Salmon, L.; Gatard, S.; Ciganda, R.; Hernandez, R.; Ruiz, J.; Astruc, D. Sodium Borohydride Stabilizes Very Active Gold Nanoparticle Catalysts. *Chem. Commun.* **2014**, *50*, 14194−14196.
(60) Stewart, M. E.; Anderton, C. R.; Thompson, L. B.; Maria, J.; Gray, S. K.; Rogers, J. A.; Nuzzo, R. G. Nanostructured Plasmonic Sensors. *Chem. Rev.* **2008**, *108*, 494−521.
(61) Farzinpour, P.; Sundar, A.; Gilroy, K. D.; Eskin, Z. E.; Hughes, R. A.; Neretina, S. Altering the Dewetting Characteristics of Ultrathin Gold and Silver Films Using a Sacrificial Antimony Layer. *Nanotechnology* **2012**, *23*, 495604.
(62) Xia, Y.; Gilroy, K. D.; Peng, H. C.; Xia, X. Seed-Mediated Growth of Colloidal Metal Nanocrystals. *Angew. Chem., Int. Ed.* **2017**, *56*, 60−95.
(63) Koczkur, K. M.; Mourdikoudis, S.; Polavarapu, L.; Skrabalak, S. E. Polyvinylpyrrolidone (PVP) in Nanoparticle Synthesis. *Dalt. Trans.* **2015**, *44*, 17883−17905.
(64) Al-Johani, H.; Abou-Hamad, E.; Jedidi, A.; Widdifield, C. M.; Viger-Gravel, J.; Sangaru, S. S.; Gajan, D.; Anjum, D. H.; Ould-Chikh, S.; Hedhili, M. N.; Gurinov, A.; Kelly, M. J.; El Eter, M.; Cavallo, L.; Emsley, L.; Basset, J. M. The Structure and Binding Mode of Citrate in the Stabilization of Gold Nanoparticles. *Nat. Chem.* **2017**, *9*, 890−895.
(65) Smith, A. M.; Johnston, K. A.; Crawford, S. E.; Marbella, L. E.; Millstone, J. E. Ligand Density Quantification on Colloidal Inorganic Nanoparticles. *Analyst* **2017**, *142*, 11−29.
(66) Ha, J.-M.; Solovyov, A.; Katz, A. Postsynthetic Modification of Gold Nanoparticles with Calix[4]arene Enantiomers: Origin of Chiral Surface Plasmon Resonance. *Langmuir* **2009**, *25*, 153−158.
(67) Smith, G. C. Evaluation of a Simple Correction for the Hydrocarbon Contamination Layer in Quantitative Surface Analysis by XPS. *J. Electron Spectrosc. Relat. Phenom.* **2005**, *148*, 21−28.
(68) Kimling, J.; Maier, M.; Okenve, B.; Kotaidis, V.; Ballot, H.; Plech, A. Turkevich Method for Gold Nanoparticle Synthesis Revisited. *J. Phys. Chem. B* **2006**, *110*, 15700−15707.
(69) Turkevich, J.; Stevenson, P. C.; Hillier, J. A Study of the Nucleation and Growth Processes in the Synthesis of Colloidal Gold. *Discuss. Faraday Soc.* **1951**, *11*, 55−75.
(70) Gómez-Lahoz, C.; García-Herruzo, F.; Rodríguez-Maroto, J. M.; Rodríguez, J. J. Cobalt(II) Removal from Water by Chemical Reduction with Sodium Borohydride. *Water Res.* **1993**, *27*, 985−992.
(71) Ohnishi, H.; Kondo, Y.; Takayanagi, K. UHV Electron Microscope and Simultaneous STM Observation of Gold Stepped Surfaces. *Surf. Sci.* **1998**, *415*, L1061−L1064.
(72) Grzeschik, R.; Schäfer, D.; Holtum, T.; Küpper, S.; Hoffmann, A.; Schlücker, S. On the Overlooked Critical Role of the pH Value on the Kinetics of the 4-Nitrophenol $NaBH_4$-Reduction Catalyzed by Noble-Metal Nanoparticles (Pt, Pd, and Au). *J. Phys. Chem. C* **2020**, DOI: 10.1021/acs.jpcc.9b07114.
(73) Graf, C.; Vossen, D. L. J.; Imhof, A.; Van Blaaderen, A. A General Method to Coat Colloidal Particles with Silica. *Langmuir* **2003**, *19*, 6693−6700.
(74) Moran, C. H.; Rycenga, M.; Zhang, Q.; Xia, Y. Replacement of Poly(vinyl pyrrolidone) by Thiols: A Systematic Study of Ag Nanocube Functionalization by Surface-Enhanced Raman Scattering. *J. Phys. Chem. C* **2011**, *115*, 21852−21857.

https://dx.doi.org/10.1021/acscatal.0c02759
ACS Catal. 2020, 10, 10040−10050